Fuel cell module control based on Switched/Time-Based Adaptive Super-Twisting Algorithm: design and experimental validation.

Anderson J.L., Moré J.J., Puleston P.F. and Costa-Castelló R.

Abstract—**Fuel cells have emerged as a sound promising technology for their application in emissions-free generation systems. Their high efficiency, reliability and clean energy make these electrochemical devices specially suitable for manifold applications such as transportation, stationary generation and portable devices. In view of the inherent complexity of this technology, the fuel cell control play a fundamental role to guarantee stability and high performance against system uncertainties and disturbances. Regarding this, sliding mode control has proven to be a powerful technique for the design of robust controllers for generation systems involving fuel cells. However, its discontinuous control action gives rise to some undesired effects when applied to real non-ideal systems, being control chattering usually the main drawback. In this framework, the paper presents the design and experimental implementation of a fuel cell module control via a Switched/Time-Based Adaptive Super-Twisting Algorithm evolving from the original ideas proposed by Pissano *et al.*. The designed algorithm is evaluated in a experimental platform of an hybrid generation system based on a commercial 1.2kW fuel cell. The proposed controller exhibits a low value of chattering and similar robustness features compared to traditional Super-Twisting Algorithm.**

Index Terms—**Adaptive Algorithm; Fuel Cells; Hybrid generation systems; Renewable Energies; Sliding Mode; Super-Twisting Algorithm**

I. Introduction

Proton-Exchange Membrane Fuel Cells (PEM-FCs) produce electricity through the conversion of the chemical energy of hydrogen, with water and heat as by-products. In view of its free pollution emission and high power density, this technology has acquired large interest in reducing dependence on fossil-fuel based generation. Moreover, particularly due to their scalability features, reduced weight and low operation temperature, the PEM-FCs are been development for several applications, such as portable devices, power system generation and, specially, transport industry [?]. However, they are complex devices and their optimization remains a challenge for advanced control systems [?].

From an electrical view point, FCs can be analysed as a nonlinear voltage source with a strong dependency on load condition and, additionally, on temperature and pressure changes. These drawbacks force their integration into a power conditioning system, comprising a Fuel Cell Module (FCM) designed to safeguard the FC and to increase the performance of the overall system [?]. Furthermore, in order to satisfy a variable power demand, the FCM is usually considered operating with an auxiliary Energy Storage System (ESS), connected together trough a common DC bus (see Fig. 1).

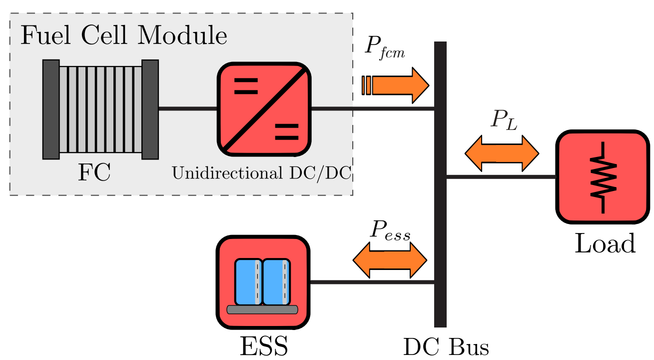

Fig. 1. Schematic of an hybrid power system based on FCM.

In this context, the Sliding Mode Control (SMC) strategies raised special interest for their application in power systems involving Fuel Cells [?] [?]. These control systems allow to overcome the low performance of traditional linear controllers, particularly in those applications with a wide operating range and strong nonlinearities, such as FCMs [?]. Furthermore, the presence of disturbances and system uncertainties makes the design of robust controllers mandatory to guarantee stability and high performance in the entire operation range.

However, problems may arise in Sliding Mode (SM) controlled systems when high frequency oscillations, commonly referred as chattering, becomes significantly important. Those oscillations are caused by the discontinuous nature of the SM control action, in combination with non-ideal (real) conditions, such as finite switching frequency or/and unmodelled system dynamics [?]. In view of that, the overall behaviour of conven-

This research was funded by ANPCyT PICT N2015-2257 Control, Electrnica e Instrumentacin: Aplicaciones en Energas Alternativas y Bioingeniera, LEICI, Fac. Ingeniera, UNLP. 20162019; CONICET PIP 112-2015-0100496CO Electrnica de potencia y sistemas de control avanzado aplicados a fuentes de energa no convencionales, LEICI, Fac. Ingeniera, UNLP. 20162019 and UNLP Proyect 11/I217 Electrnica de potencia y sistemas de control avanzado aplicados a fuentes de energa no convencionales, LEICI, Fac. Ingeniera, UNLP. 20162019.

Additionally, this work has been partially funded by the Spanish national project DOVELAR ref. RTI2018-096001-B-C32 (MCIU/AEI/FEDER, UE). This work is supported by the Spanish State Research Agency through the Mara de Maeztu Seal of Excellence to IRI (MDM-2016-0656).

Anderson J.L., Moré J.J. and Puleston P.F. are with the Instituto de investigación en Electrónica, Control y Procesamiento de señales (LEICI), FI UNLP - CONICET, La Plata, Argentina (e-mail: jorgeluis.anderson@ing.unlp.edu.ar).

Costa-Castelló R. is with the Institut de Robòtica i Informàtica industrial (IRI), CSIC-UPC, Barcelona, España.

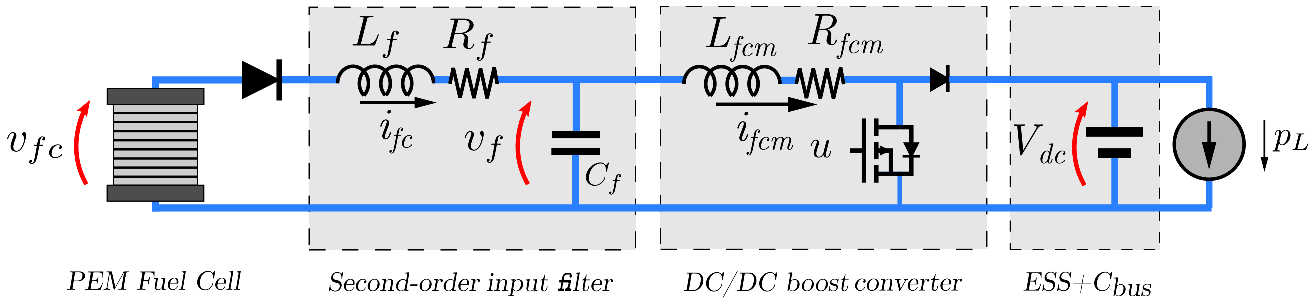

Fig. 2. Scheme of the electrical model for fuel cell module.

tional SM controllers could be deteriorated, mainly affecting their performance and robustness.

For the last decades, a major concern has been the design of different SMC-based algorithms to reduce system chattering and, at the same time, maintain the robust features and finite time convergence of conventional SMC [?]. In that context, the Second Order Sliding Mode (SOSM) control has emerged as an interesting alternative, existing today several algorithms developed in the literature. One of the most employed structures are SubOptimal Algorithm (SOA) [?], Twisting Algorithm (TA) and Super-Twisting Algorithm (STA) [?], the latter being directly applicable to relative degree one systems.

Although the implementation of SOSM controllers is usually simple and of relatively low online computational cost, main efforts need to be carried out on their design stage. Particularly, in practice, it is sometimes required to oversized the SOSM gains, in order to allow the controller to deal with large, but not necessarily frequent, disturbances. Such beefed up control efforts would undermine the chattering amelioration in non-ideal, real SM controlled systems.

Nowadays, the Adaptive SOSM (A-SOSM) algorithms have been introduced to overcome the above issues. These structures allow to preserve robustness features of SOSM strategies, achieving system stability in disturbed conditions, while reducing chattering through an online adjustment of their control parameters. Several adaptation mechanisms for SOSM algorithms have been successfully developed in the literature (for instance, [?], [?], [?], [?], [?]), some of them with excellent experimental results (e.g., [?], [?]).

In particular, in latest years, Pisano *et al.* [?] have proposed a novel mechanism to deal with the finite switching frequency presented in real SM in engineering systems. This time-based new approach employs the zero-crossing count of the sliding variable on a time window. Thereupon, the system operation over the real SM regime is established when such count is big enough to satisfy a given SM existence criterion. Then, the time-based adaptation logic will reduce the SOSM controller gains as long as such criterion holds. Conversely, if the system leaves the operation over the real SM regime, the SOSM gains will be rapidly increased to avoid unstable system conditions.

The above time-based adaptation approach is specially suitable for its practical implementation in the fuel cell module under study. In the first place, the adaptation algorithm does not required extra information, it only uses the sliding variable, without further measurement of other fuel cell signals nor parameters. On the other hand, its low computation cost and simple programming structure provide an enhanced control performance, without enlarging the complexity of the real-time implementation of the fuel cell controller.

Currently, this novel mechanism has been studied and developed, for SOSM Twisting [?] and SubOptimal Algorithms [?], with direct application to relative degree 2 systems. In [?], this strategy was employed for a SOSM Twisting algorithm to control of a two-wheeled vehicle. In [?], the proposed mechanism was designed for a SOSM-SOA control in robotic application. In [?], a receding horizon adaptation time window was incorporated for the control of a doubly-fed induction generator based wind turbine. Nevertheless, as far as the authors know, no experimental validation of the time-based adaptive SOSM algorithms was assessed to control of power generation systems.

In this framework, the main contributions of this paper are focused on two aspects. Firstly, based on the adaptive approach presented in [?], a Switched/Time-Based Adaptive STA (STBA-STA) is developed to control a Fuel Cell Module. This control structure allows its direct application on relative degree one systems, as the FCM under consideration. Secondly, the proposed fuel cell STBA-STA controller is implemented and assessed on an experimental Hybrid Generation System (HGS), based on a 1.2kW commercial fuel cell. The Adaptive STA controlled system performance and robustness is successfully compared to both, a conventional SOSM STA structure with fixed gains and a linear controller.

II. Electrical Model for Fuel Cell Module

In this section, the electrical model of the Fuel Cell Module operating as a core of an hybrid generation system is developed. The FC is connected to an unidirectional DC/DC converter, adapting the low and variable voltage level of the FC to the common DC Bus as shows Fig. 2. With this structure, the FC system power flow streams from the fuel cell stack to the load, supplying the requested main power and preserving the integrity of the power stack.

To proceed with the experimental evaluation, the common DC Bus is supposed to be regulate by an Energy Storage System (ESS), emulated through an electronic load. The storage system will be responsible of providing transient power requirements, assisting the FC in satisfying the peak-load demand and recovering exceeding energy.

A. Proton-exchange membrane fuel cell

A well-known electrical model (see Fig. 4) for the voltage variation of a FC composed by N_{stack} cells, considering regulated temperatures and partial pressures, is given by [?]:

$$\begin{cases} v_{fc} & = E_{nl} - v_{dl} - R_{ohm} i_{fc} \\ C_{dl} \dot{v}_{dl} & = C_{dl} \left(\dot{v}_{act} \left(i_{fc} \right) + \dot{v}_{conc} \left(i_{fc} \right) \right) \end{cases} \tag{1}$$

where E_{nl} is the open circuit voltage, R_{ohm} represents the linear losses, the electrical capacitance C_{dl} describes the double layer effect, and v_{act} and v_{conc} are highly nonlinear functions of the fuel cell current i_{fc}.

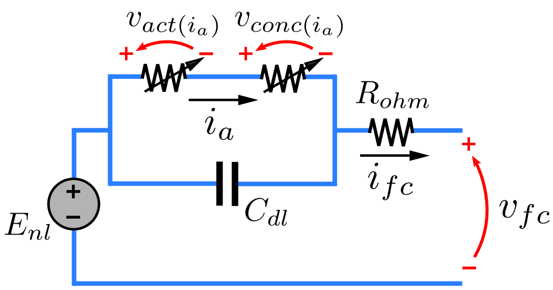

Fig. 3. Electrical model of a Proton-exchange membrane fuel cell.

The overvoltage v_{act} models the starting voltage drop due to the activation losses through the Tafel Equation. This effect is most important at low current. Meanwhile the concentration losses v_{conc} represent losses due to changes in reactant concentrations, which produce a reduction in their partial pressures and generate an significantly voltage drop at high current. Both terms can be described by the nonlinear expressions:

$$v_{act} \left(i_{fc} \right) = N_{stack} A_t ln \left(i_{fc} \right), \tag{2}$$

$$v_{conc} \left(i_{fc} \right) = N_{stack} m \exp \left(n i_{fc} \right) \tag{3}$$

with A_t the slope of the Tafel equation and m and n empirical coefficients. The electrical model described in (1) has been successfully applied to the power system analysis that involves FCs, and it is extensively used in the literature [?] [?].

B. Power conditioning system based on boost converter.

The FCM topology is based on an unidirectional boost DC/DC power converter. Additionally, a second order low-pass filter is implemented at the fuel cell output. This filter helps to mitigate the high frequency components of the switching current, which degrade FC's wellness. The common DC Bus is considered perfectly regulated by the Energy Storage System to a constant value V_{bus}. The above is made under the assumption of fast transient response of ESS with respect to the FC dynamic.

Under the above consideration, the state model for the studied Fuel Cell Module is given by:

$$\dot{x} = f_{(x)} + g_{(x)} u \tag{4}$$

where the state vector x is equal to

$$x = \begin{bmatrix} x_1 & x_2 & x_3 \end{bmatrix}' = \begin{bmatrix} i_{fc} & v_f & i_{fcm} \end{bmatrix}' \tag{5}$$

and

$$f_{(x)} = \begin{bmatrix} -\dfrac{R_f}{L_f} x_1 - \dfrac{1}{L_f} x_2 + \dfrac{1}{L_f} v_{fc}(x_1) \\ \dfrac{1}{C_f} x_1 - \dfrac{1}{C_f} x_3 \\ \dfrac{1}{L_{fcm}} x_2 - \dfrac{R_{fcm}}{L_{fcm}} x_3 \end{bmatrix}, \tag{6}$$

$$g_{(x)} = \begin{bmatrix} 0 \\ 0 \\ \dfrac{V_{dc}}{L_{fcm}} \end{bmatrix}. \tag{7}$$

with u is the duty cycle, with $0 < u_{min} < u < 1$.

III. Switched/Time-Based Adaptive SOSM Super-Twisting Algorithm.

In this section, the design of the Switched/Time-Based Adaptive Super-Twisting Algorithm (STBA-STA) for the FCM is carried out. The development of the proposed controller is performed from a traditional Super-Twisting Algorithm with Fixed Gains (STA-FG). For this reason, first, the basic concepts of SOSM control design are given, introducing the conventional STA-FG structure.

Then, the time-based adaptation mechanism is developed as a top layer of the control system. In this way, the Super-Twisting gains are modified trough the proposed law. Additionally, in order to guarantee the stability of the controlled system, a necessary stability condition is detailed. Finally, some design considerations are given for the proposed FCM control parameters.

A. Basic concepts for Second Order Sliding Mode (SOSM) control design.

The fuel cell module control is designed to manage the electrical current of the FCM supplied to the common DC bus. This design is carried out by defining the FCM current tracking reference $i_{fcm,r}$, established by an external supervisor control. By means of Sliding Mode theory, this control objective can be expressed trough the sliding variable σ as:

$$\sigma(x) = x_3 - i_{fcm,r}. \tag{8}$$

The power tracking will be addressed by designing a control system that drive and maintain σ and $\dot{\sigma}$ to zero, i.e. to the sliding manifold:

$$\mathbb{S} = \{x \in R^3 : \sigma(x) = \dot{\sigma}(x) = 0\}, \tag{9}$$

in finite time. Then, by combining the expression of σ in (8) and the control-affine structure of system (4)-(7), it can be easily shown that the first and second derivative of σ, $\dot{\sigma}$ and $\ddot{\sigma}$, take the mathematical forms:

$$\dot{\sigma}(x) = \Phi(x) + \Gamma(x) u \tag{10}$$

$$\ddot{\sigma}(x,u) = \varphi(x,u) + \Gamma(x)\dot{u} = \Gamma(x)\left[\eta(x,u) + \dot{u}\right] \tag{11}$$

with

$$\Phi(x) = \frac{d\sigma(x)}{dx} f(x) - \dot{i}_{fcm,r}, \tag{12}$$

$$\Gamma(x) = \frac{d\sigma(x)}{dx} g(x), \tag{13}$$

$$\varphi(x,u) = \dot{\Phi}(x) + \dot{\Gamma}(x)u \tag{14}$$

and

$$\eta(x,u) = \frac{\varphi(x,u)}{\Gamma(x)}. \tag{15}$$

At this point, it should be noticed that if $\Gamma(x) \neq 0$, which is commonly satisfied for FCM normal operation conditions, the control action u presents a relative degree one with respect to the sliding variable σ.

B. Super-Twisting Algorithm with Fixed Gains

A well-known algorithm that can lead and maintain system trajectories to the second-order sliding manifold $\mathbb{S}$, described in (9), in finite time is the Super-Twisting Algorithm with Fixed Gains given by [**?**]:

$$u = -\alpha(t)|\sigma(x)|^{1/2}\text{sign}(\sigma(x)) + \omega \tag{16}$$

$$\dot{\omega} = -\beta(t)\text{sign}(\sigma(x)). \tag{17}$$

with

$$\beta(t) = \beta_0 \quad and \quad \alpha(t) = \alpha_0. \tag{18}$$

This SOSM controller allows to be applied directly in relative degree one systems, as the studied topology. Additionally, mainly due to its continuous control action, it achieves a significantly amelioration of chattering with respect to traditional first-order sliding mode controllers.

It can be proved that if the system functions Γ and φ of (13) and (14) are bounded by:

$$|\varphi(x,u,t)| \leq F \text{ and } 0 < G_m \leq \Gamma(x) \leq G_M, \tag{19}$$

for the entire FCM operation range, the control parameters β_0 y α_0, of constants values for the STA-FG, can be designed to satisfy the stability conditions:

$$\beta_0 > \frac{F}{G_m} \quad \text{and} \quad \alpha_0^2 > \frac{2}{G_m^2}\frac{(G_m\beta_0 + F)^2}{(G_m\beta_0 - F)}. \tag{20}$$

Then the STA-FG will deliver the system (4)-(7) to $\mathbb{S}$ in finite time and, once reach it, it will remain over it [**?**].

As was commented previously, the constants F, G_m and G_M, bounds of the controlled system, are obtained by considering the worst case for system perturbations. In this way, in practical implementations, the parameters β_0 and α_0 are usually oversized for the purpose of guaranteeing the system stability over the entire operation range, and against the possible system variations and disturbances. This, in addition with the conservative conditions defined in (20) and the limited switching frequency of power converters, leads to an inevitable increasing of the resulting *chattering* of the controlled system, which may be inadmissible.

C. Switched/Time-Based Adaptive Super-Twisting Algorithm

The previous motivates the development of the switched/time-based adaptation mechanism for the STA parameters adjustment. As was explained earlier, the proposed algorithm computes the zero crossing number of the sliding variable $N(\sigma)$ and compares it with the threshold value $\tilde{N} > 0$.

If $N(\sigma)$ is greater than $\tilde{N}$, the controlled system is considered operating on the real SOSM regime $\mathbb{S}_R$ and, then, the reduction of the parameters α and β in ec. (18) is performed. The parameter amelioration is sustained as long as the condition remains fulfilled. On the contrary, if due to this reduction, the zero crossing number $N(\sigma)$ becomes too small, the adaptation mechanism will rapidly increase the STA parameters, allowing system trajectories reach $\mathbb{S}_R$ again.

The measurement of the zero number crossing $N_k(\sigma)$, for instant $k \in \mathbb{N}_0$, is computed for each overlapping time interval $\mathcal{T}_k$:

$$\mathcal{T}_k = [kT_a - T, kT_a], \quad T = \tilde{k}T_a \tag{21}$$

with T_a the actuation period equal to switching period in the FCM power converter. The window size T is proportional to T_a with positive integer $\tilde{k}$.

Therefore, the Super-Twisting control gains in (18) are redefined as:

$$\beta(t) = \beta[k], \quad \alpha(t) = \varepsilon\sqrt{\beta[k]}, \quad \varepsilon > 0. \tag{22}$$

where $\beta[k]$ value is updated at each period T_a, remaining constant during time interval $t \in [kT_a, (k+1)T_a]$. Thus, depending on the number of zero crossing $N_k(\sigma)$, $\beta[k]$ is modified by following the adaptation law:

$$\beta[k] = \begin{cases} \max\left(\beta[k-1] - \Lambda T_a, \beta_{\text{min}}\right), & \text{if } N_{k-1}(\sigma) \geq \tilde{N} \\ \min\left(\beta[k-1] + \Gamma T_a, \beta_{\text{max}}\right), & \text{if } N_{k-1}(\sigma) < \tilde{N} \end{cases} \tag{23}$$

for $k \geq \tilde{k}$, Λ, Γ, β_{min}, β_{max} and $\tilde{N} \geq 3$ positive constants.

Additional, for practical purposes, in order to obtain the first measure of $N_{\tilde{k}-1}(\sigma)$, it is implemented an initialization period for $k \leq \tilde{k} - 1$ during which $\beta[k]$ remains constant:

$$\beta[k] = \beta[0], \quad \text{with } \beta_{\text{min}} \leq \beta[0] \leq \beta_{\text{max}}. \tag{24}$$

1) Stability condition for the proposed STBA Super-Twisting Algorithm: Next, it will be enunciated a preposition to establish a sufficient condition for the stability of the proposed control system.

Let the system of (4) with control affine structure, which zero dynamics are stable over the sliding manifold $\mathbb{S}$. In addition, let the functions Γ, φ and η, defined on (13), (14) and (15), respectively, be bounded by:

$$|\varphi(x,u,t)| \leq F, \quad 0 < G_m \leq \Gamma(x) \leq G_M \tag{25}$$

and

$$\left|\frac{d}{dt}\eta(t,\cdot)\right| \leq P, \tag{26}$$

for some positive constants F, G_m, G_M and P. Then, if the control parameters of the algorithm Switched/Time-Based

Adaptive Super-Twisting Algorithm (STBA-STA) presented in (22)-(24), are designed to satisfy:

$$0 < \beta_{\min} \leq \beta_{\max} = \gamma \frac{F}{G_m}, \quad \gamma > 1 \tag{27}$$

$$\varepsilon^2 > \frac{4}{G_m} \frac{(\gamma+1)}{(\gamma-1)} \tag{28}$$

and

$$\Gamma > \Lambda + (\tilde{k}+2)P, \tag{29}$$

the system trajectories will converge to the real second-order sliding manifold:

$$\mathcal{S}_R = \left\{ x \in \mathbb{R}^3 : |\sigma(x)| < \mu_1, |\dot{\sigma}(x)| < \mu_2 \right\} \tag{30}$$

in finite time.

Due to its deduction is analogue to MDSO Twisting and Suboptimal algorithms [?] [?], the formal proof of the proposition will not carry out in the present paper. Nevertheless, the algorithm stability is based on the idea that if the number of zero crossings $N_k(\sigma)$ is smaller than the threshold value $\tilde{N}$, the adaptation algorithm will increase β value until reach, in the worst case, to $\beta_{\max}$. In such situation, because $\beta_{\max}$ and ε satisfy the stability conditions (27) and (28), equivalent to STA-GF stability conditions in (20), the system trajectories will eventually return to $\mathbb{S}$. In this way, the zero crossings number $N_k(\sigma)$ will start to increase it until reach condition $N_k(\sigma) > \tilde{N}$ again.

On the other way, through the condition (26), which establish some notions about speed variation of σ, it can be obtained the condition (29). This condition defines a relation between parameters Γ and Λ which guarantee that, if condition $N_k(\sigma) > \tilde{N}$ is broken in some time, the controlled system will go back to satisfy it in time period less to the window length T.

2) Design of STBA-STA control parameters.: The design procedure of the control parameters implies finding the bounds F, G_m, G_M and P, defined in (27)-(29). In order to guarantee the control robustness, they must be computed considering possible disturbances and system parameter uncertainties. However, finding these constants analytically may result in highly complex equations that leads to very conservative bounds. In view of this, in the present work, the values of F, G_m, G_M and P are obtained employing a numerical procedure.

The Fig. 4 illustrates the numerical approach, where it is displayed one set of functions φ, Γ and $\dot{\eta}$ employed for the control parameters tuning. The system trajectories have been generated by considering system parameters variations of 20% and sinusoidal bus voltage disturbances of 2.5% bus amplitude. This bus disturbances consist in four frequency steps from 0 to 4Hz, identical to the ones employed in the experimental evaluation (see Sec. IV-B).

After an exhaustive simulation analysis, evaluating the system operation for diverse disturbance conditions and parameters variations, the values of F, G_m, G_M and P are computed. Even though numerically obtained, the control parameters of (22)-(24 should be experimentally adjusted in order to attain the desired system chattering and robustness properties.

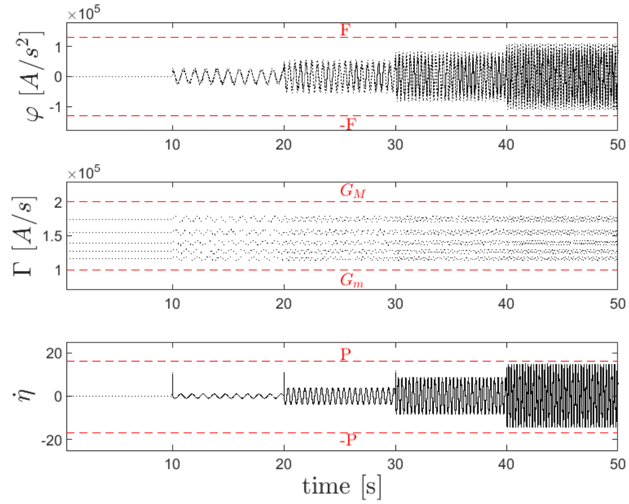

Fig. 4. Set of system functions φ, Γ and $\dot{\eta}$ for diverse trajectories.

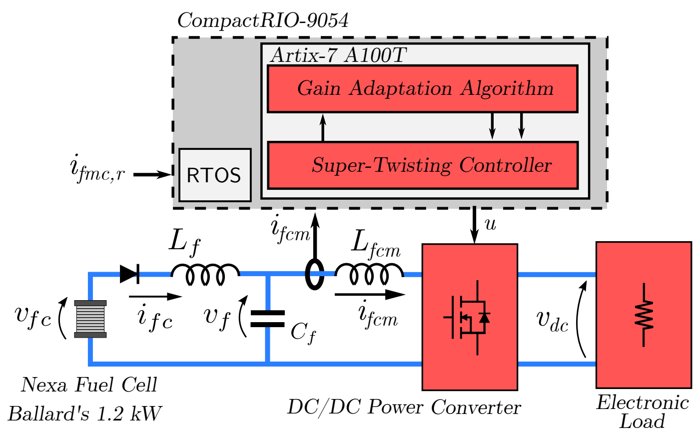

Fig. 5. Experimental setup of the Fuel Cell Module prototype.

IV. Experimental results.

In this section, the experimental results of the Fuel Cell Module control are presented. The experimental setup is shown in Fig. 5, where are detailed the involved subsystems.

The employed FC is a Ballard's 1.2 kW Nexa© Fuel Cell Power Module [?], which has a nominal voltage of 26V at rated power. The employed algorithms are developed into the National Instruments© platform cRIO-9054 [?]. The NI device incorporates an FPGA Artix-7 family, which allows its configuration through Labview©.

In order to compare the proposed STBA-STA strategy with traditional controllers, in similar operating conditions, the common DC Bus is emulated through an electronic load [see MODEL]. This configurable load is settled to regulate the bus voltage v_{dc}, allowing to incorporate controlled system disturbances for the FCM evaluating process.

Additionally to the developed STBA-STA algorithm, the performance of the controlled FCM is also evaluated for a STA with Fixed Gain and a traditional PI linear controllers. The linear controller was adjusted using the heuristic ZieglerNichols tuning method, which allowed to obtain similar time responses with respect the designed SOSM controls.The experimental system and controls parameters are detail in table I.

TABLE I
PARAMETERS OF THE EXPERIMENTAL 1.2KW FUEL CELL MODULE CONTROL.

FCM and STBA-STA parameters					
$V_{fc,nom}$	$26V$	L_f	$140\mu H$	L_c	$160\mu H$
$I_{fc,nom}$	$46A$	C_f	$2200\mu F$	f_s	$20kHz$
$P_{fc,nom}$	$1.2kW$	V_{dc}	$70V$	P	18
β_{min}	0.1	Λ	$3.00e^5 kW/s$	F	$1.2e5A/s^2$
β_{max}	0.23	Γ	$2.50e^5 kW/s$	G_m	$1e5A/s$
$\tilde{N}$	4	T	$0.025s$	G_M	$2e5A/s$

Two experimental tests will be carry out to study the performance of the Fuel Cell Module. The first one is intended to evaluate the control reference tracking when the controlled system operates in absence of disturbances. The second one will test the control systems robustness against bus voltage perturbation.

A. Control systems tracking to $i_{fcm,r}$ reference in absence of disturbance.

The current reference $i_{fcm,r}$ tracking in normal operating conditions is performed using a ramp reference profile. In this situation, the FCM is considered operating without bus disturbances, in order to evaluate common system time response for all controllers. Due to practical constrains in FC dynamics behaviour, the slope of tracking signal is limited to $10A/s$, representing a more exigent value than is typically employed in FC applications [?]. The time response of the three controllers are displayed in Fig. 6. As can be appreciated, both SOSM controllers achieves an acceptable tracking of the imposed signal reference. However, as it is well-known, the linear control cannot perfectly track a ramp reference, presenting an important error at slope changes.

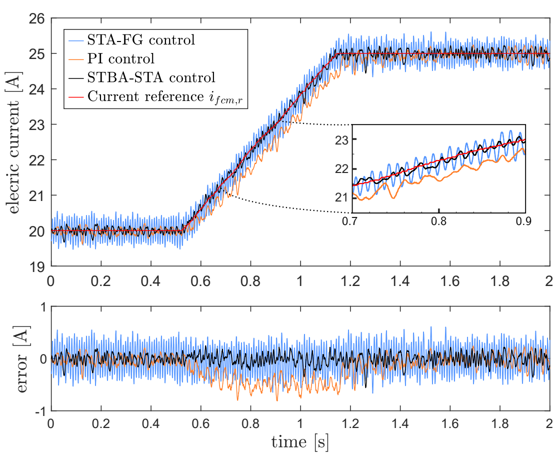

Fig. 6. Ramp reference tracking for all control systems in absence of bus disturbance.

In view of the low value of β of the proposed STA-AG strategy, consistent with the absence of system perturbations, the resulting chattering becomes naturally smaller than the STA-FG controller. Moreover, the STA-AG chattering presents similar amplitudes than the linear control while, at the same time, the proposed controller assures the perfect tracking of $i_{fcm,r}$.

B. Control system evaluation under bus voltage disturbances.

Now, the proposed strategy will be evaluated in presence of bus disturbances, allowing to prove the adaptation mechanism for the control parameter β. To this end, a sinusoidal perturbation of 2.5% bus amplitude is emulated by the electronic load, while it is settled a fixed value for the signal reference. The amplitude value of the sinusoidal is chosen considering technical constrains of the electronic load.

The FCM test consists in four frequency steps from 0 to $4Hz$, where the required control effort is gradually increased. The time response of the three controllers can be observed in Fig. 7 together with the bus voltage variation.

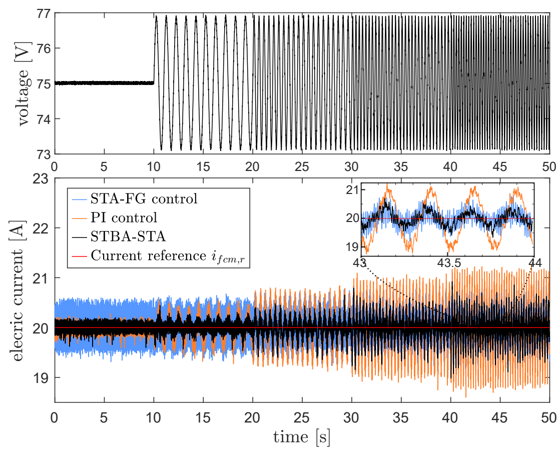

Fig. 7. Control systems time response in presence of bus disturbance.

As in the previous test, in absence of disturbance, the STA-AG chattering remains smaller than conventional STA-FG. However, as the frequency disturbance is increased, the small value of β is not sufficient to reject it and the number of zero crossings begins to be reduced (see Fig. 8). In this way, the proposed adaptation mechanism rapidly increases STA parameters, achieving disturbance rejection and guaranteeing controlled system robustness. On the other hand, the linear controller cannot reject the bus disturbance and presents a significantly reduction of its control performance.

It can be appreciated how the STA-AG chattering is increased as β increases as well. This behavior is naturally expected because of the controller needs a greater control effort to reject the perturbation. The control actions of both SOSM controllers are displayed in Fig. 9.

Finally, it should be noticed that, even though β_{min} exhibit a great control performance when system operates without disturbance, this value is not designed to be able to reject bus perturbation in conventional STA-FG. This is appreciated in more detail in Fig. 10, where the above STA-AG time response is compared with a STA-FG with β_{min}. As is expected, STA-FG cannot reject bus disturbance and the controlled systems presents an significantly reduction of its performance.

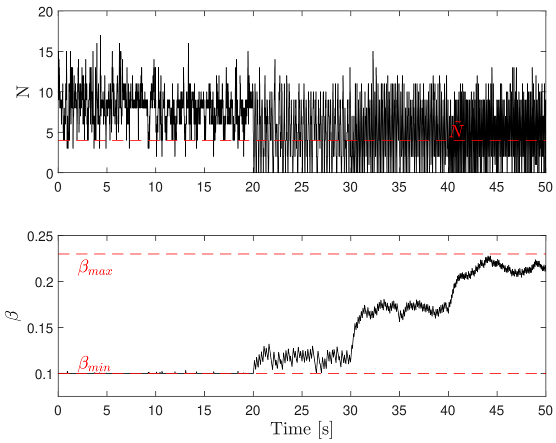

Fig. 8. Time response of STA-AG control parameters.

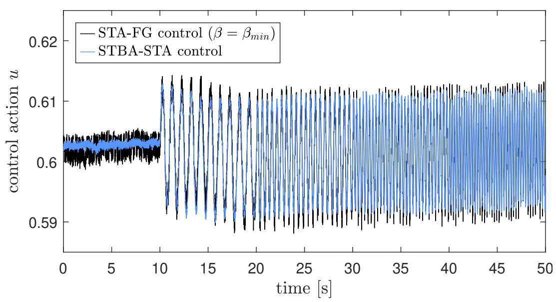

Fig. 9. Time response of the control action for both sliding mode controllers.

V. Conclusions.

This paper proposed the design and experimental validation of a Fuel Cell Module control based on a Switched/Time Based Adaptive Super-Twisting Algorithm. The presented adaptation law was based on Pisano et al. algorithm, which is relied on real sliding mode concept. In order to guarantee system stability for the proposed controller, a necessary condition for its stable operation was given.

The experimental validation was implemented on an hybrid power generation system with a commercial PEM Fuel Cell as its main core. The employed Fuel Cell was a Nexa Ballard FC with a rate power of 1.2kW. Furthermore, the associated energy storage system was emulated via an electronic load, allowing desired bus disturbance conditions to be imposed.

The performance of the proposed STA with gain adaptation was compared with a conventional STA with Fixed Gain and a PI linear controllers on two experimental tests. In the first setup, a ramp tracking reference was generated in order to evaluate all controllers in absence of perturbation. The second test was designed to assess control system robustness in presence of sinusoidal bus disturbance with variable frequency.

In both experimental tests, the STBA-STA controller exhibited a low value of chattering in absence of system perturbation. Moreover, in presence of bus disturbance, the proposed controller achieved similar robustness features with respect to traditional STA-FG. In this way, the presented adaptation mechanism resulted being a very effective tool to implement

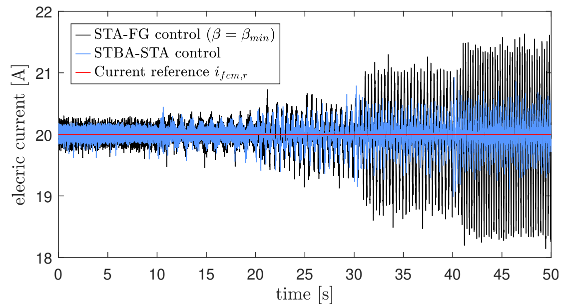

Fig. 10. Time response of STA-FG for $\beta = \beta_{min}$.

in power systems that involves fuel cells, allowing to increase system performance while it guarantee the required system robustness.